NeuroImage: Clinical 36 (2022) 103223

Contents lists available at ScienceDirect

NeuroImage: Clinical

journal homepage: www.elsevier.com/locate/ynicl

The effect of time delay for magnetic resonance contrast-enhanced scan on imaging for small-volume brain metastases

Mingming Chen [a,b], Pengcheng Wang [b], Yujie Guo [a], Yong Yin [a], Lizhen Wang [a], Ya Su [a], Guanzhong Gong [a,c,*]

[a] Department of Radiation Physics, Shandong First Medical University Affiliated Cancer Hospital, Shandong Cancer Hospital and Institute (Shandong Cancer Hospital), Jinan 250117, China
[b] College of Radiology, Shandong First Medical University & Shandong Academy of Medical Sciences, Jinan 250117, China
[c] Department of Engineering Physics, Tsing Hua University, Beijing 100084, China

ARTICLE INFO

Keywords:
Brain metastases
Delayed-time
Maximum diameter
Small-volume
MRI

ABSTRACT

Purpose: To study the effect of different enhancement timings of magnetic resonance (MR) on small-volume brain metastases (BM) visualisation and provide a basis for the contour of tumour targets.
Method: We prospectively enrolled 101 patients with BM who received radiotherapy. All patients underwent computed tomography (CT) and MR simulations. Contrast-enhanced MR scans at 1, 3, 5, 10, 18, and 20 min after injection of contrast medium were performed. The tumour target was determined on MR images at different enhancement times, and the differences of tumour target volume, maximum diameter, and MR signal intensity were compared.
Results: (1) Of the 453 metastatic lesions, 24 (5.2 %) were not detected at 1 min and 8 (1.8 %) were not detected at 3 min; however, all metastases were detected after 5 min. The volume and maximum diameter of the 28 (6.2 %) metastases were stable at any time. (2) The average volume of metastatic lesions at 1, 3, 5, 10, 18, and 20 min was 0.09 cm^3, 0.10 cm^3, 0.12 cm^3, 0.12 cm^3, 0.13 cm^3, and 0.13 cm^3, respectively. Compared to 1 min, BM volume at other times increased by 13.1 %, 21.5 %, 31.6 %, 39.6 %, and 41.7 %, and the difference between the maximum and minimum volumes was statistically significant ($p < 0.05$). (3) The distribution of the maximum ratio of tumours to white matter mean signal intensity at different times were 39.6 %, 20 %, 14.6 %, 8.0 %, 10.4 %, and 10 %, respectively.
Conclusion: The visualisation of small-volume BM was significantly different at different enhancement times. Our results suggest that multi-timing enhancement scans for small-volume BM should be implemented and that scanning at >10 min is essential.

1. Introduction

Brain metastases (BM) are the most common intracranial tumours in adults, accounting for up to 80 % of primary tumours in patients with BM from lung cancer, breast cancer, and melanoma (Sacks and Rahman, 2020; Kim and Kim, 2021; Jablonska et al., 2022). Recently, the incidence of BM has increased due to improvements in tumour treatment efficacy and prolonged patient survival (Saria et al., 2015). Approximately 30 %-50 % of patients with BM die of uncontrolled and recurrent intracranial lesions, and BM has become the main cause of death in patients with malignant brain tumours (Achrol et al., 2019).

Presently, BM are mainly treated with comprehensive treatments such as surgery, radiotherapy, chemotherapy and biological targeted therapy. Specifically, radiotherapy has played an irreplaceable role (Putora et al., 2020). Radiotherapy is one of the most effective methods for treating BM; for small-volume BM, a single high-dose SRS has achieved promising clinical outcomes (Hessen et al., 2020; Mulford et al., 2021). Accurate quantification of BM and accurate contour of gross tumour targets (GTV) are critical for patient risk stratification, appropriate radiotherapy planning, and prognosis; however, accurate contour of GTV to evaluate tumour targeting is a challenging task (Engh et al., 2007; Dupic et al., 2021).

* Corresponding author at: Department of Radiation Physics, Shandong First Medical University Affiliated Cancer Hospital, Shandong Cancer Hospital and Institute (Shandong Cancer Hospital), Jinan 250117, China.
E-mail address: gongguanzhong@yeah.net (G. Gong).

https://doi.org/10.1016/j.nicl.2022.103223
Received 17 May 2022; Received in revised form 7 September 2022; Accepted 3 October 2022
Available online 5 October 2022

Contrast-enhanced (CE) magnetic resonance imaging (MRI) is the standard imaging technique for determining the number, size, and location of BM, and studies have shown that MR using gadolinium (Gd) contrast agents is currently the gold standard for identifying and characterising BM (Essig et al., 2012). Since tumour metastasis and growth can cause different degrees of blood–brain barrier (BBB) damage, paramagnetic Gd contrast agents show significant visual differences when infiltrating perivascular tissue, showing a time-dependent effect on MR enhancement—especially on small-volume BM (Hattingen et al., 2017). The timing of image acquisition after contrast agent injection is also an important factor that affects the accuracy and intensity of MRI signals (Tsao et al., 2012).

The main problems are missed diagnosis and unclear boundary of small-volume BM, which cannot accurately define the tumour target, resulting in off-target phenomenon and treatment failure (Kirkpatrick et al., 2015). An accurate and repeatable display of tumour volume on MRI is reliable for radiotherapy planning design and tumour response assessment (Yip and Aerts, 2016). Therefore, optimising the imaging timing between contrast agent administration and imaging sequence is a key step in improving the diagnostic sensitivity of CE MRI for small-volume BM and accurately determining the tumour target area.

This study investigated the influence of enhanced MR on the visualisation of small-volume BM at different times, aiming to determine the optimal timing for detection and display of small-volume BM and provide a basis for delineating the target area for radiotherapy.

2. Materials and methods

2.1. Patient information

A total of 101 patients with BM who received radiotherapy at the Cancer Hospital Affiliated to Shandong First Medical University from February to October 2021 were prospectively enrolled. Among them, 48 were males (age range, 42–80 years; average age, 60.8 years) and 53 were females (age range, 36–81 years; average age, 56.6 years). The primary tumour types included 84 lung cancers, 14 breast cancers, and 3 oesophageal cancers.

3. Methods

3.1. CT simulation

All patients were fixed with thermoplastic films and scanned using a Philips Brilliance Big Bore CT locator (Philips, Amsterdam, The Netherlands) with 3 mm thickness and at 3-mm interval in the supine position.

3.2. MR simulation

After the CT simulation was completed, all patients were placed in the same body position, and fixation method was used to obtain MR simulation images using a GE 3.0 T superconducting MR scanner (Discovery 750 W, GE Healthcare, Chicago, IL, USA) equipped with a 6-channel head coil. All patients underwent 3D T1-weighted gradient-echo brain volume imaging (T1 BRAVO) enhanced scans at 1, 3, 5, 10, 18, and 20 min after intravenous injection of a Gd-containing contrast agent.

The enhanced scan parameters were as follows: TR = 8.5 ms, TE = 3.2 ms, matrix = 256 × 256, FOV = 256 mm × 256 mm, and slice thickness = 1 mm, layer number = 50–52, and T1 sequence image acquisition time was 1 min 55 s^{-1} min 58 s. The Gadoteric Acid Meglumine Salt Injection was injected with an MR injection system (MEDRAD® Spectris Solaris EP, Bayer, Leverkusen, Germany) at the rate of 2 mL/s and dose of 0.2 mL/kg, and then flushed with 20 mL saline.

3.3. Delineation of tumour target

The lesion was defined as a mass with low-to-medium signal intensity on T1 and focal parenchymal abnormal enhancement on CE-T1 scan, with higher signal intensity than the normal brain parenchyma. The MRIs of all patients were imported into the MIM Maestro (7.1.7, Cleveland, OH, USA) software where the images of six timings were fused and registered. Without considering the time sequence of delayed enhancement and patients' clinical conditions, three radiologists manually delineated the tumour target area and counted the number of lesions on MR images at different time points of enhancement together, using T2Flair images as reference. Then, a certain volume of white matter was delineated at the same position in the central semiovale region of images at their corresponding time points. In case of indeterminate lesions, the images were reviewed by a senior radiologist. Each determined tumour and white matter were defined as regions of interest (ROIs) to be analysed to assess whether the ROIs of each timing corresponded accurately.

3.4. Acquisition of tumour target information

First, the number of BM with a maximum diameter of <1 cm in all enrolled patients were counted six times after administration. Then, the volume, maximum diameter, and average signal intensity of each metastatic lesion and average signal intensity in the white matter were calculated from the data automatically generated by the MIM software.

3.5. Statistical analysis

The volume, maximum diameter, and average signal intensity of metastatic lesions, as well as the volume and maximum diameter of metastatic lesions at 10–18 min and 18–20 min after contrast administration, were assessed using IBM SPSS (version 26.0, Armonk, NY, USA) statistical software. With $P < 0.05$ indicated significant difference.

4. Results

4.1. Overview of the BM

The maximum diameter of the metastases at the 1 min time point was used as the inclusion criterion, thus metastases >1.0 cm at 1 min were excluded. Eventually, a total of 453 metastases with a maximum diameter <1 cm were sketched in 101 patients; 24 (5.2 %) of these were not detected at 1 min, 8 (1.8 %) were not detected at 3 min, and all 453 metastases were detected after 5 min. The volume and maximum diameter of 28 (6.2 %) metastases did not change at any time (Fig. 1).

4.2. Comparison of metastatic volumes at different times

The average volumes of all metastases at 1, 3, 5, 10, 18, and 20 min were 0.09 cm^3, 0.10 cm^3, 0.12 cm^3, 0.12 cm^3, 0.13 cm^3, and 0.13 cm^3, respectively. Compared to 1 min, the volumes at 3, 5, 10, 18, and 20 min increased by 13.1 %, 21.5 %, 31.6 %, 39.6 %, and 41.7 %, respectively (Table 1, Fig. 2).

The frequencies of the maximum volume at different times were 6 (1.4 %), 19 (4.5 %), 32 (7.5 %), 104 (24.5 %), 147 (34.6 %), and 117 (27.5 %), respectively. The total proportion of distribution in 10–20 min was 86.6 %, with the distribution the largest at 18 min. The volume differences between 10 and 18 min and 18 and 20 min were statistically significant ($p < 0.05$). However, 28.5 % of the metastatic lesions decreased at 18–20 min, 28.9 % increased (change rate of metastatic lesions >10 %), and the remaining metastatic lesions showed no change (Table 2 and Fig. 3).

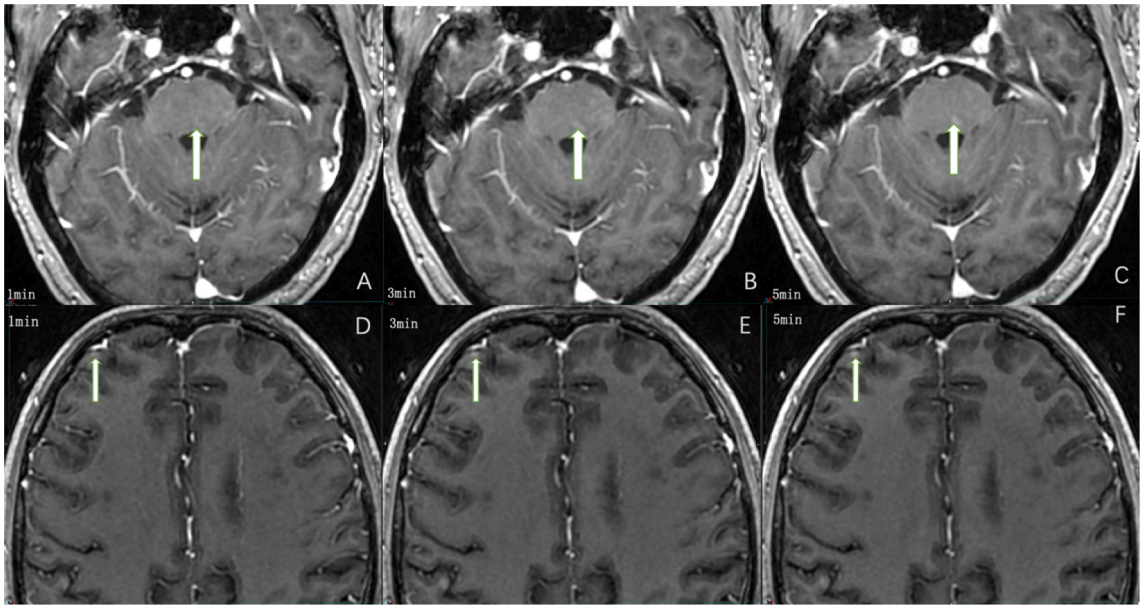

Fig. 1. A, B, and C show no obvious lesions at 1 and 3 min after injection of Gd, respectively, and significant enhancement at 5 min. Figures D, E, and F show no obvious lesions at 1 min after injection of Gd, but with significant enhancement at 3 and 5 min.

Table 1
Mean changes of maximum diameter and volume at different times.

Category	Time					
	1 min	3 min	5 min	10 min	18 min	20 min
Maximum diameter (cm)	0.75 ± 0.15	0.77 ± 0.16	0.79 ± 0.18	0.81 ± 0.18	0.83 ± 0.19	0.83 ± 0.20
Volume (cm^3)	0.09 ± 0.05	0.10 ± 0.06	0.12 ± 0.13	0.12 ± 0.14	0.13 ± 0.15	0.13 ± 0.15

4.3. Comparison of the maximum diameter of metastases at different time points

The average maximum diameters of the metastases at 1, 3, 5, 10, 18, and 20 min were 0.75 cm, 0.77 cm, 0.79 cm, 0.81 cm, 0.83 cm, and 0.83 cm, respectively. Compared to 1 min, the maximum diameters at 3, 5, 10, 18, and 20 min increased by 2.4 %, 2.9 %, 7.2 %, 9.6 %, and 9.8 %, respectively (Table 1).

The frequencies of the maximum diameter at different times were 3 (0.7 %), 13 (3.1 %), 28 (6.6 %), 94 (22.1 %), 162 (38.1 %), and 125 (29.4 %) (Fig. 3). The maximum frequency at 18 min and the difference in maximum diameter at 10 and 18 min were statistically significant ($p < 0.05$), while the difference between the maximum diameter at 18 and 20 min was not statistically significant ($p > 0.05$). However, the maximum diameter of metastases from 18 to 20 min in 45.7 % of patients showed an increasing trend; 37.5 %, showed a downward trend; and 16.8 %, showed no change. The changing trends of metastasis volume and maximum diameter were similar; both increased until 18 min

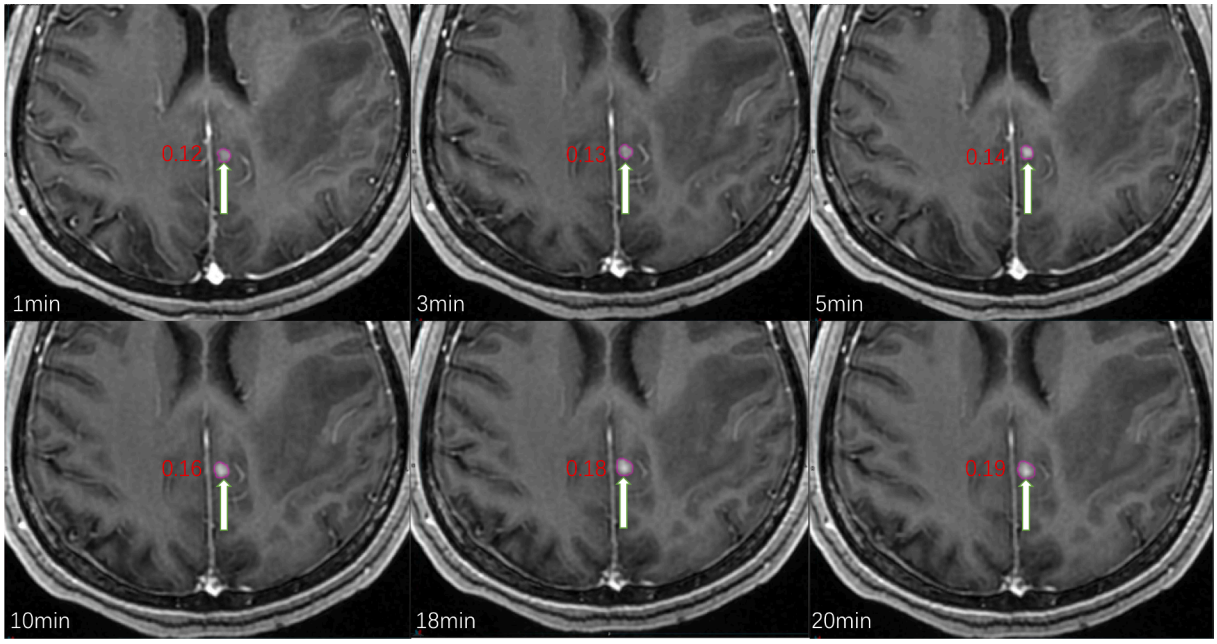

Fig. 2. Changes in volume (cm^3) and signal intensity of metastases in a patient at different times.

Table 2
Comparison of maximum diameter and volume at different time points.

Category	Time 1 min	3 min	5 min	10 min	18 min	20 min
Maximum diameter (cm)	3(0.7 %)	13 (3.1 %)	28 (6.6 %)	94(22.1 %)	162 (38.1 %)	125 (29.4 %)
Volume (cm^3)	6(1.4 %)	19 (4.5 %)	32 (7.5 %)	104 (24.5 %)	147 (34.6 %)	117 (27.5 %)

and then stabilised with time delay (Fig. 4). Differences between the maximum and minimum values were statistically significant ($p < 0.05$; Table 1 and Fig. 5).

4.4. Analysis of changes in tumour signal intensity

The average signal intensity of a tumour at 1, 3, 5, 10, 18, and 20 min were 1417.8, 1477.3, 1458.8, 1403.1, 1382.5, and 1386.6, respectively. The signal intensity peaked at 3 min and then decreased with increasing time delay. Compared to 3 min, the signal intensities at 1, 5, 10, 18, and 20 min decreased by 4.2 %, 1.3 %, 5.3 %, 6.9 %, and 6.5 %, respectively, and the change was the greatest at 18 min (Table 3).

The frequencies of the maximum tumour average signal intensity at different time points were 34.3 %, 24.7 %, 22.7 %, 4.9 %, 8.2 %, and 7.5 %, respectively. The peak value of the distribution was at 1 min and showed a slight upward trend when it decreased to 10 min. The difference between the maximum and minimum tumour signal intensities were statistically significant ($P < 0.05$, Fig. 6).

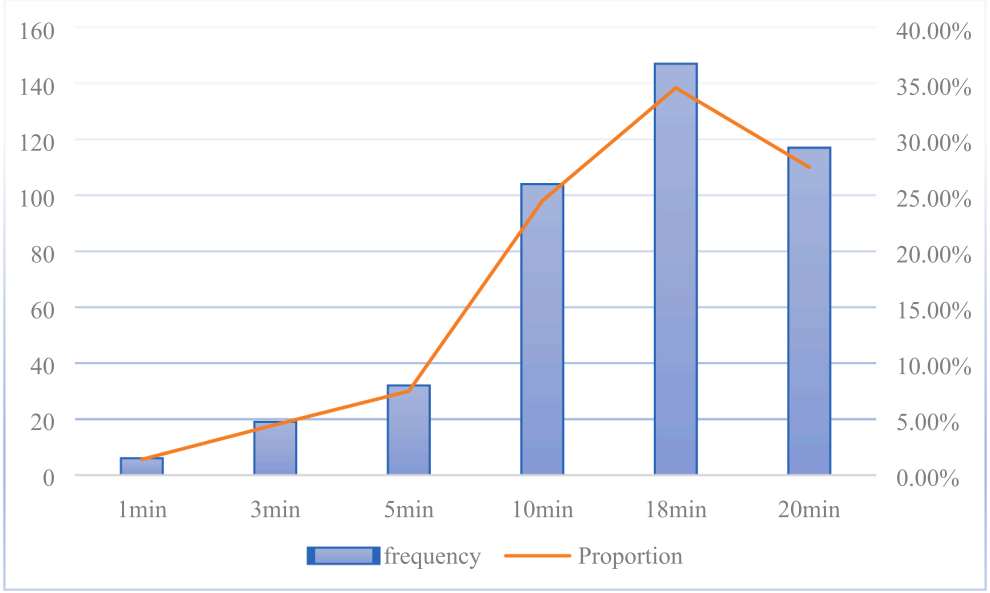

Fig. 3. The frequency of the maximum tumour volume at different times.

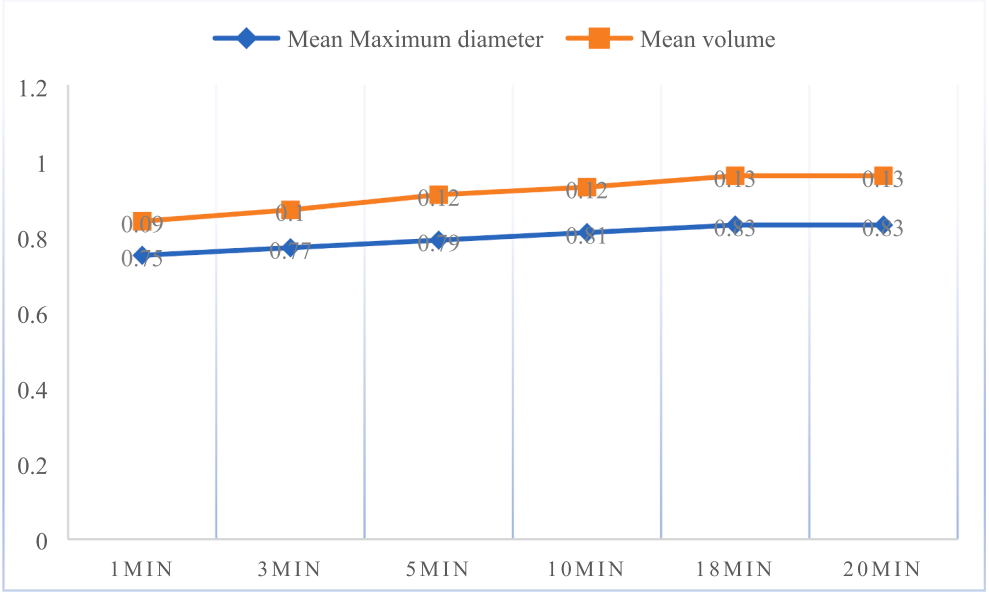

Fig. 4. Mean changes in tumour maximum diameter and volume with time.

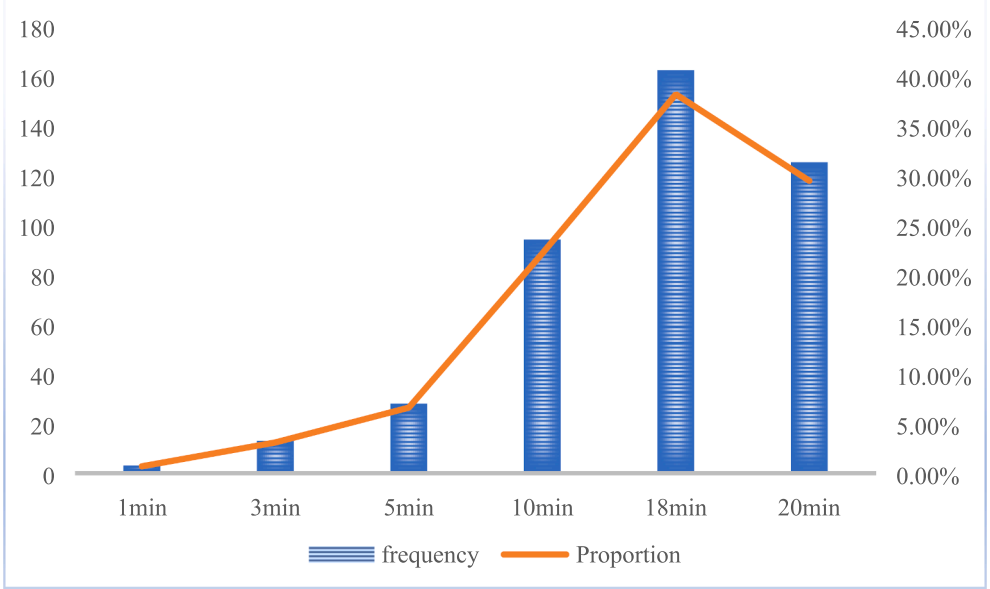

Fig. 5. Frequency changes of the maximum tumour diameter at different time points.

Table 3
The mean change and distribution ratio of tumour signal intensity at different time points.

Category	Time 1 min	3 min	5 min	10 min	18 min	20 min
Proportion	34.3 %	24.7 %	22.7 %	4.9 %	8.2 %	7.5 %
Mean	1417.8 ± 328.7	1477.3 ± 373.7	1458.8 ± 344.3	1403.1 ± 334.9	1382.5 ± 332.6	1386.6 ± 333.4

4.5. Analysis of changes in white matter signal intensity

The average signal intensity means of white matter at different time points were 1192.6, 1196.7, 1194.0, 1163.0, 1163.4, and 1157.9, respectively. Although the signal intensity of white matter did not change significantly between 1 and 5 min, the highest signal intensity was the same as that of tumours at 3 min. Compared with signal intensity at 3 min, the average signal intensity decreased by 2.5 %, 2.9 %, and 3.4 % at 10, 18, and 20 min, respectively. The change trend was similar to that of the tumour; however, the signal intensity of the tumour was higher than that of the white matter (Fig. 6).

The frequencies of the maximum average signal intensity of white matter at different times were 19.4 %, 28.6 %, 46.9 %, 0, 2 %, and 3.1 %, and the distribution of the maximum value peaked at 5 min. Although the distribution ratio of the signal intensity between the tumour and white matter is not consistent, >70 % of the maximum signal intensity was concentrated within the first 1–5 min. The difference between the maximum and minimum values of white matter signal intensity was statistically significant ($p < 0.05$).

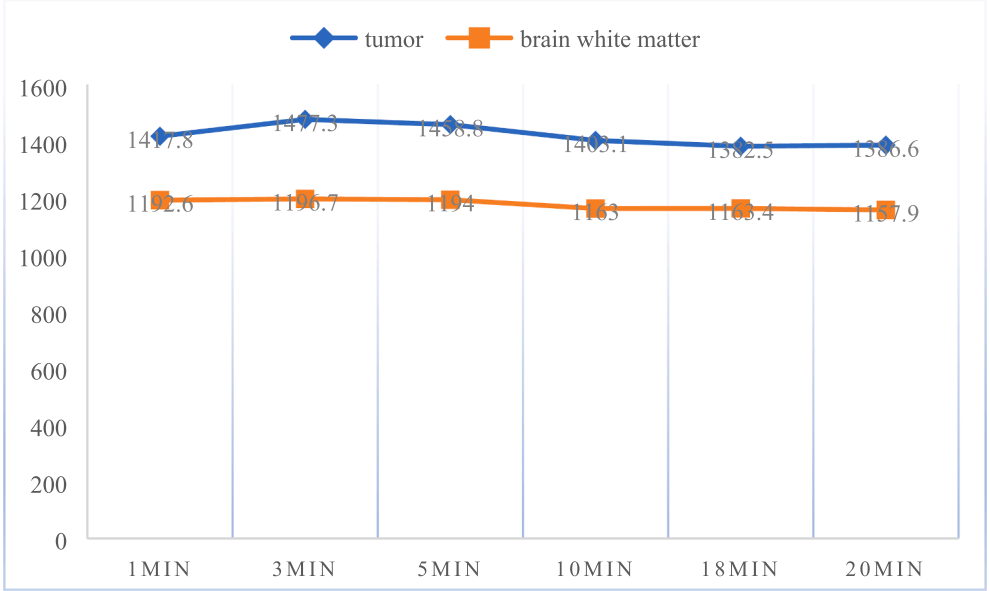

Fig. 6. The mean change trend of tumour and white matter average signal intensity at different time points.

4.6. Analysis of changes in the tumour to white matter signal intensity ratio

The frequencies of the maximum tumour to white matter average signal intensity ratio at different times were 39.6 %, 20 %, 14.6 %, 8 %, 10.4 %, and 10 %, respectively. Overall, the distribution of the tumour to white matter signal ratios was approximately the same as the distribution of the tumour signal intensity values. The peak value of the signal intensity was mainly concentrated at 1 min, and the signal intensity first decreased with time, and then slightly increased after 10 min. However, the distribution peak of the maximum value of the white matter signal intensity was observed at 5 min (Fig. 7).

5. Discussion

This study quantified the changes in small-volume BM with different MR enhancement timings and confirmed significant differences in the visualisation of small-volume BM with different enhancement timings and showed the inability of traditional fixed-timing enhancement scans to fully characterise BM on imaging. Therefore, in this study, our results showed the combination of multi-time enhanced scanning in the detection of small-volume BM, delineation of tumour target areas, and a delay of >10 min as the necessary sequence.

Imaging diagnosis of BM relies mainly on BBB destruction on CE scanning findings. While the contrast medium cannot pass through the complete BBB, but the pathologically damaged BBB area is significantly enhanced, resulting in the accumulation of contrast medium in the extracellular space of the affected tissue and an increase in longitudinal relaxation. Compared to healthy tissues, the capillary permeability of BM is abnormally high; therefore, the signal intensity is increased in T1-weighted images (Heye et al., 2014). Delayed imaging may be an effective way to improve adequate tumour visualisation because it allows more time for the contrast agent to penetrate the destroyed BBB and for neovascularisation within the metastases. Some studies have shown that the surface of small blood vessels of micrometastases may not allow a large dose of contrast agent to penetrate using a kinetic method simultaneously, and the contrast agent's penetrative ability has a certain time dependence (Lüdemann et al., 2005). The difference in the display of tumour boundaries in our results also supports this postulate.

In this study, 5.2 % of the metastases were not visualised at 1 min due to their small volume, and the degree of BBB damage was not as obvious, resulting in a longer time for the contrast medium to enter the tissue. A total of 1.7 % of the metastases were not visualised at 3 min, indicating that conventional MR enhanced 3 min scanning was also insufficient; however, all metastases were visualised after 5 min. Therefore, for the detection and delineation of small-volume BM, 5 min delineation should be used as the initial sequence. Cohen-Inbar et al. (2016) investigated the influence of three acquisition timings—post Gd contrast agent injection—on the detection of BM and reported that the time-delayed T1WI sequence has significantly higher sensitivity for detecting micro-volume BM, which is consistent with the results of our study.

Enhanced timing also had a significant effect on the ability to visualise the volume of small-volume BM. In this study, compared to 10 min, 1, 3, and 5 min underestimated the volume by 31.6 %, 18.5 %, and 10.1 %, respectively. However, small-volume BM are generally treated with SRS, which has more stringent requirements for the display boundary and volume of BM. The loss of volume during imaging may cause some tumour areas to not be included in the tumour target because the imaging is incomplete and the radiation dose is insufficient, resulting in radiotherapy failure. Although the volume of BM in this study remained changed after 10 min, the trend slowed. Compared to 10 min, the volume increases at 18 and 20 min were only 8 % and 10 %, respectively; thus, an enhancement of > 10 min should be considered a necessary sequence in the radiotherapy of small-volume BM. This was confirmed in Kang et al.'s results (Kang et al., 2018). Qiu et al. (2016) elucidated the best time to delineate the border of glioma in mice, based on MR delayed enhancement, and confirmed that the timing of enhancement has a significant effect on tumour delineation; these results were also shown in the present study.

Simultaneously, we analysed the signal intensity of the tumours and white matter and found that tumour signal intensity and ratio of tumour to white matter signal intensity showed a decreasing trend with each time delay. However, the signal intensity of white matter showed an increase in trend first until 5 min, followed by a decrease with further delay, indicating that contrast medium penetration changed dynamically with the delay of enhancement time; this is consistent with Jeonet al.'s findings (Jeon et al., 2014). This result may also be due to angiogenesis as a key factor in tumour growth and metastasis, and even contrast media that normally cannot penetrate normal blood vessels can pass through tumour vessels more quickly, resulting in increased differences leading to rapid entry and dissipation of the contrast medium (Lee et al., 2022). Although signal intensity was greatest at 1 min, it is

Fig. 7. Change of maximum distribution ratio of the tumour, white matter, and tumour to white matter signal intensity ratio.

not recommended as a reference sequence to determine small-volume BM targets because some tumours are still not fully visualised. However, this changed at 10 min, suggesting that the tumours may have entered the dynamic equilibrium state of contrast medium infiltration and elimination, consistent with the maximum diameter and volume of the tumour. Therefore, we recommend that a sequence with a delay exceeding 10 min should be considered.

This study has limitations. None of the patients in this study received radiotherapy; therefore, we were unable to compare dosimetry and elucidate the efficacy of radiotherapy. Notably, delayed enhancement beyond 20 min has not been studied; however, based on our results, we speculate that a delay beyond 20 min has little effect on the diagnosis and target delineation of BM.

In conclusion, our study found that a delayed scan post-contrast enhancement of MR visualised a more accurate radiotherapy target for patients with BM who were to receive radiotherapy, confirming that delaying the time of contrast enhancement of MR could improve the diagnostic sensitivity for small-volume BM. In order to reduce the omission of metastases and the accurate delineation of the tumour target, this study suggested that multi-time enhanced scanning should be performed in BM patients receiving radiotherapy with a delay of >10 min as a necessary sequence.

6. Ethics approval

This study involved human participants and was approved by the Shandong First Medical University Affiliated Cancer Hospital: IRB 2022005008.

7. Data availability statement

All data relevant to the study are included in the article.

Funding

This study was supported by the Start-up fund of Shandong Cancer Hospital (YYPY2020-016), and the Key Research and Development Program of Shandong Major Science & Technology Innovation Project (2021SFGC0501).

CRediT authorship contribution statement

Guanzhong Gong: Methodology, Conceptualization, Funding acquisition, Software, Formal analysis, Project administration, Supervision, Writing - review & editing.

Declaration of Competing Interest

The authors declare that they have no known competing financial interests or personal relationships that could have appeared to influence the work reported in this paper.

Data availability

No data was used for the research described in the article.

References

Achrol, A.S., Rennert, R.C., Anders, C., Soffietti, R., Ahluwalia, M.S., Nayak, L., et al., 2019. Brain metastases. Nat. Rev. Dis. Primers 5, 5.

Cohen-Inbar, O., Xu, Z., Dodson, B., Rizvi, T., Durst CR.,Mukherjee S,, et al., 2016. Time-delayed contrast-enhanced MRI improves detection of brain metastases: a prospective validation of diagnostic yield. J. Neurooncol. 130, 485–494.

Dupic, G., Brun, L., Molnar, I., Leyrat, B., Chassin, V., Moreau, J., et al., 2021. Significant correlation between gross tumor volume (GTV) D98% and local control in multifraction stereotactic radiotherapy (MF-SRT) for unresected brain metastases. Radiother. Oncol. 1.

Engh, J.A., Flickinger, J.C., Niranjan, A., Amin, D.V., Kondziolka, D.S., Lunsford, L.D., 2007. Optimizing intracranial metastasis detection for stereotactic radiosurgery. Stereotact. Funct. Neurosurg. 85, 162–168.

Essig, M., Anzalone, N., Combs, S.E., Dörfler, À., Lee, S.K., Picozzi, P., et al., 2012. MR imaging of neoplastic central nervous system lesions: review and recommendations for current practice. AJNR Am. J. Neuroradiol. 33, 803–817.

Hattingen, E., Müller, A., Jurcoane, A., Mädler, B., Ditter, P., Schild, H., et al., 2017. Value of quantitative magnetic resonance imaging T1-relaxometry in predicting contrast-enhancement in glioblastoma patients. Oncotarget 8, 53542–53551.

Hessen, E., Nijkamp, J., Damen, P., Hauptmann, M., Jasperse, B., Dewit, L., et al., 2020. Predicting and implications of target volume changes of brain metastases during fractionated stereotactic radiosurgery. Radiother. Oncol. 142, 175–179.

Heye, A.K., Culling, R.D., Valdés Hernández Mdel, C., 2014. Thrippleton MJ, Wardlaw JM. Assessment of blood-brain barrier disruption using dynamic contrast-enhanced MRI. A systematic review. Neuroimage Clin. 6, 262–274.

Jablonska, P.A., Fong, C.H., Kruser, T., Weiss, J., Amy Liu, Z., Takami, H., et al., 2022. Recommended first-line management of brain metastases from melanoma: A multicenter survey of clinical practice. Radiother. Oncol. 168, 89–94.

Jeon, J.Y., Choi, J.W., Roh, H.G., Moon, W.J., 2014. Effect of imaging time in the magnetic resonance detection of intracerebral metastases using single dose gadobutrol. Korean J Radiol. 15, 145–150.

Kang, K.M., Choi, S.H., Hwang, M., Yoo, R.E., Yun, T.J., Kim, J.H., et al., 2018. Application OF Synthetic MRI for direct measurement of magnetic resonance relaxation time and tumor volume at multiple time points after contrast administration: preliminary results in patie. Korean J. Radiol. 19 (4), 783–791.

Kim JS, Kim IA., 2021. Evolving treatment strategies of brain metastases from breast cancer: current status and future direction. Ther Adv Med Oncol. 12: 1758835920936117.

Kirkpatrick, J.P., Wang, Z., Sampson, J.H., McSherry, F., Herndon 2nd, J.E., Allen, K.J., et al., 2015. Defining the optimal planning target volume in image-guided stereotactic radiosurgery of brain metastases: results of a randomized trial. Int. J. Radiat. Oncol. Biol. Phys.

Lee, J.Y., Lee, K.S., Seo, B.K., Cho, K.R., Woo, O.H., Song, S.E., et al., 2022. Radiomic machine learning for predicting prognostic biomarkers and molecular subtypes of breast cancer using tumor heterogeneity and angiogenesis properties on MRI. Eur. Radiol. 32, 650–660.

Lüdemann, L., Grieger, W., Wurm, R., Wust, P., Zimmer, C., 2005. Quantitative measurement of leakage volume and permeability in gliomas, meningiomas and brain metastases with dynamic contrast-enhanced MRI. Magn. Reson. Imaging. 23, 833–841.

Mulford, K., Chen, C., Dusenbery, K., Yuan, J., Hunt, M.A., Chen, C.C., et al., 2021. A radiomics-based model for predicting local control of resected brain metastases receiving adjuvant SRS. Clin. Transl. Radiat. Oncol. 29, 27–32.

Putora, P.M., Fischer, G.F., Früh, M., Califano, R., Faivre-Finn, C., Van Houtte, P., et al., 2020. Treatment of brain metastases in small cell lung cancer: Decision-making amongst a multidisciplinary panel of European experts. Radiother. Oncol. 2020 (149), 84–88.

Qiu, L., Zhang, F., Shi, Y., Bai, Z., Wang, J., Li, Y., et al., 2016. Gliomas: motexafin gadolinium-enhanced molecular MR imaging and optical imaging for potential intraoperative delineation of tumor margins. Radiology 279, 400–409.

Sacks, P., Rahman, M., 2020. Epidemiology of Brain Metastases. Neurosurg. Clin. N. Am. 31, 481–488.

Saria, M.G., Piccioni, D., Carter, J., Orosco, H., Turpin, T., Kesari, S., 2015. Current Perspectives in the management of brain metastases. Clin J Oncol Nurs. 19 (4), 475–479.

Tsao, M.N., Rades, D., Wirth, A., Lo, S.S., Danielson, B.L., Vichare, A., et al., 2012. International practice survey on the management of brain metastases. Third International Consensus Workshop on Palliative Radiotherapy and Symptom Control. Clin Oncol (R Coll Radiol).

Yip, S.S., Aerts, H.J., 2016. Applications and limitations of radiomics. Phys. Med. Biol. 61, R150–R166.